An optimized control strategy using multivariable modulation and reactive power exchange cancellation for a multi-active bridge (MAB) converter

Rebecca Tarraf, Sébastien Carcouet, David Frey, Sylvain Leirens, Xavier Maynard, Yves Lembeye

AN OPTIMIZED CONTROL STRATEGY USING MULTIVARIABLE MODULATION AND REACTIVE POWER EXCHANGE CANCELLATION FOR A MULTI-ACTIVE BRIDGE (MAB) CONVERTER

Rebecca Tarraf [1*], Sébastien Carcouet [1], David Frey [2], Sylvain Leirens [1], Xavier Maynard [3], Yves Lembeye [2]

[1]Université Grenoble Alpes, CEA, Leti, F-38000 Grenoble, France
[2]Université Grenoble Alpes, G2Elab, CNRS, F-38000 Grenoble, France
[3]Université Grenoble Alpes, CEA, Liten, F-38000 Grenoble, France
**rebecca.tarraf@cea.fr*

Keywords: MULTI-PORT DC-DC CONVERTERS, MULTI-ACTIVE BRIDGE (MAB) CONVERTER, CONTROL STRATEGY, OPTIMIZATION, SOFT SWITCHING.

Abstract

A Multi-Active Bridge (MAB) converter is an interesting energy hub topology that has emerged in recent years. This multi-port structure has recently attracted a lot of attention, especially for applications soliciting renewable energy sources and energy storage systems. In general, the main objective of controlling a MAB converter is to manage the active power flows between its ports based on each port's requirements. However, optimizing the control of this converter can be achieved by adding another constraint, aiming to minimize the system's losses for example. In this paper, a novel optimized control strategy is proposed for a MAB converter consisting of any number of ports. This approach provides users with a choice between prioritising efficient system operation, which may result in the loss of soft switching at specific switches, or aiming for soft switching at all system switches with decreased losses, even if it leads to suboptimal efficiency. A 1KW 4-port MAB prototype is built and experimental results are provided in this paper to validate the developed theoretical study.

1 Introduction

Multi-Active Bridge (MAB) converters are multiport converters provided with intrinsic galvanic isolation. This is due to the connection of this topology's ports through a multi-winding transformer. Consequently, a MAB converter can connect several energy sources, loads and energy storage systems with different voltage levels and power ratings together, allowing multidirectional power flow between them [1]. For these reasons, MAB converters drew greater attention in recent years in many applications, especially those requiring energy storage or/and integrating renewable energy sources.

In literature, a common method for controlling a MAB converter is to fix a duty cycle of 50% on all ports' AC voltages at the transformer windings and vary the phase shifts between these voltages, also known as 'external phase shifts' of the MAB [2]–[4]. That way, the external phase shift value of each voltage will impose the power drawn from or received by its corresponding port. This method will be called "External Phase Shift Modulation" (EPS) from now on in this paper. EPS modulation is a very efficient and simple method to control the active power flow in a MAB converter when it comes to operating at nominal power. However, EPS modulation may lead to increased losses at certain operating points, such as when low power is flowing through the system or when voltage mismatches occur, because the combination of control parameters it uses is not necessarily the optimal one. Therefore, additional control parameters are needed.

In [5], the switching frequency of the MAB converter is used as the additional control parameter, along with the external phase shifts, to reduce the total system losses. However, this could lead to electromagnetic compatibility (EMC) problems and a complex passive component sizing.

The duty ratios of the ports' AC voltages, also called "Internal Phase Shifts", can also be the additional control parameters. The works in [6] and [7] used the internal and external phase shifts to control a MAB converter while minimizing its losses. However, these works represent two extreme solutions to the same problem. In [6], a Perturb and Observe (P&O) algorithm was employed in order to track the minimum RMS current point of the MAB converter. This simple control method leads to decreased conduction losses and does not require a lot of computational effort or any mathematical model of the system. However, it does not take into consideration the switching losses and can easily settle the system into a local minimum. In [7], an all-inclusive, five-variable optimization problem was developed for a MAB converter with three ports (TAB) using its generalized harmonic approximation (GHA) model. This optimization problem aims to minimize the total system losses (conduction, switching and transformer losses) while maintaining the desired power flow constraints. The optimal values of the internal and external phase shifts are the outputs of this developed problem. Although this control technique absolutely leads the system to maximum efficiency, the computational effort it requires is enormous so it cannot be

executed in real time. Lookup tables were used to store pre-calculated control variables at specific operating points only, leading to suboptimal operation at operating points that are not included in the lookup table.

This paper proposes a new solution that lies between these two extremes. Therefore, an efficiency-optimization control method is proposed, aiming to decrease the conduction and switching losses of a MAB converter, with a tolerable amount of computational effort and without the risk of operating in a local minimum. Conduction losses are decreased by limiting the amount of reactive power exchange between the ports. Switching losses are decreased by ensuring a soft switching on the ports' switches. A generalized harmonic approximation (GHA) model is established for a MAB converter with n ports to be able to predict the optimal values of the control parameters at each operating point. Experimental results are obtained using a 4-port MAB (QAB) converter prototype in order to validate the presented control strategy.

The rest of this paper is organized as follows: in Section 2, the chosen topology of the MAB converter is shown and the developed GHA model is detailed. Then, the conduction losses are stated in Section 3. In Section 4, the ZVS criteria at the different switching instants are elaborated, and their resulting losses are defined. The proposed optimization algorithm is explained in Section 5. Finally, experimental results are shown in Section 6.

2 Topology and Modelling

2.1 MAB Converter Topology

The considered MAB converter topology is presented in Fig. *1*. Each port consists of a voltage source (representing either a real power source or a load having the behaviour of a voltage source) and a classical H-bridge. L_i represents the leakage inductance of the transformer winding of port #i, which can be connected to an external series inductance.

Fig. 2 illustrates the star-delta equivalent models of the transformer, neglecting the series resistances. In the delta network, the link inductances can be calculated as follows [1]:

$$L_{ij} = \begin{cases} NA, & \forall i = j \\ L_i' + L_j' + L_i' L_j' \left(\sum_{k \neq i,j}^{n} \frac{1}{L_k'} \right), & \forall i \neq j \end{cases}$$

Parameters $L_i{}' = L_i / n_{1i}^2$ and $v_{ac,i}{}' = v_{ac,i} / n_{1i}$ are the leakage inductance and AC voltage of a port #i, respectively, referred to the reference port, which will be port #1 in this study. $n_{1i} = n_i / n_1$ is the transformer turn ratio between port #i and port #1. In Fig. *3*, the AC voltages $v_{ac,i}$ of a port #i and $v_{ac,1}$ of port #1 are represented. The external phase shift of the reference port will be considered zero ($\varphi_1 = 0$). Therefore, all the other ports are shifted with respect to this port. We denote as $\varphi_{ij} = \varphi_i - \varphi_j$ the external phase shift between port #i and port #j. The internal phase shift of a port #i is denoted as α_i and is as represented in Fig. *3*.

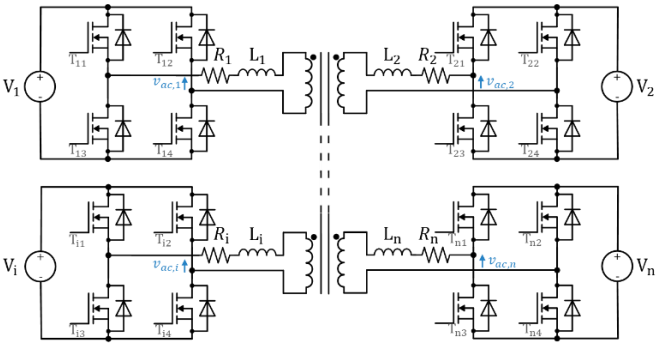

Fig. 1: Topology of a Multi-Active Bridge converter with n ports.

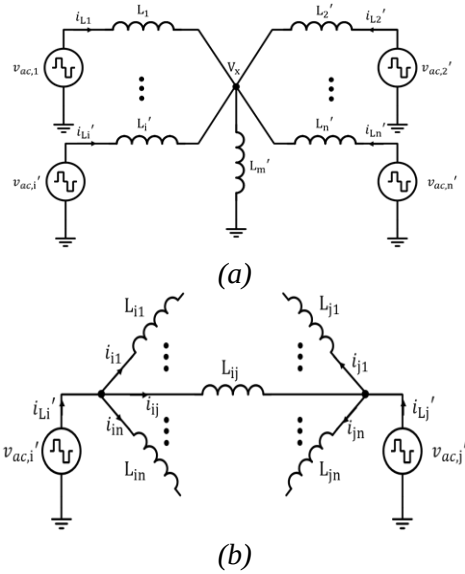

Fig. 2: Star-delta transformation of the MAB converter's transformer model: (a) Star model, (b) Delta model.

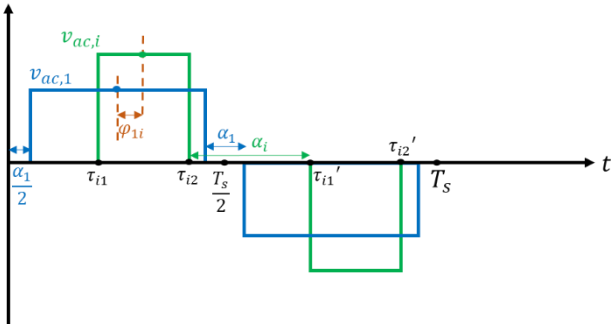

Fig. 3: AC voltages of reference port #1 and port #i with their corresponding external and internal phase shifts.

2.2 GHA model of an n-port MAB converter

In literature, many works have proposed time-domain-based modelling methods for a DAB converter (MAB with 2 ports) [8]–[10]. Nevertheless, a time-domain-based study of a MAB converter consisting of more than two ports is very complex to achieve because the number of operating modes increases dramatically when the number of ports increases. For this reason, a frequency-domain-based study would be a better

solution. In EPS modulation, the first harmonic approximation of the AC signals represents the system's behaviour accurately [2]. However, in Multiple-Phase Shift (MPS) modulation where both internal and external phase shifts are used to control the system, the first harmonic approximation fails to represent the system correctly. Consequently, a GHA model is developed for a MAB converter with n ports in this paper. The AC voltage of port #i is represented by the following infinite summation, using Fourier series expansion and Fig. *3* [11]:

$$v_{ac,i}'(t) = \frac{4V_i}{n_{1i}.\pi} \sum_{\substack{k=1 \\ k\ odd}}^{\infty} \frac{1}{k} \cos\left(k\frac{\alpha_i}{2}\right) \times \sin\left(k.(w_s t - \varphi_{1i})\right) \quad (1)$$

V_i is the DC voltage of port #i. $w_s = 2\pi f_s$ where f_s is the switching frequency of the converter. k is the harmonic order. The current flowing from port #i to port #j referred to the reference port #1 can be deduced from (1) and the delta model of (b)
Fig. 2(b) as follows:

$$i_{ij}(t) = \frac{1}{L_{ij}} \int_0^t \left(v_{ac,i}'(t) - v_{ac,j}'(t)\right) dt \quad (2)$$

$$= \frac{4}{\pi w_s L_{ij}} \sum_{\substack{k=1 \\ k\ odd}}^{\infty} \left[-\frac{V_i}{n_{1i}.k^2} \cos\left(k\frac{\alpha_i}{2}\right).\cos\left(k.(w_s t - \varphi_{1i})\right) + \frac{V_j}{n_{1j}.k^2} \cos\left(k\frac{\alpha_j}{2}\right).\cos\left(k.\left(w_s t - \varphi_{1j}\right)\right)\right]$$

Consequently, we can get the expression of the total current sourced by port #i into the other ports, referred to its own side of the transformer, as follows:

$$i_{L,i}(t) = \sum_{\substack{j=1 \\ j\neq i}}^{n} \frac{i_{ij}(t)}{n_{1i}} \quad (3)$$

n is the number of ports of the considered MAB converter.
The average active power flowing between a port #i and a port #j during a switching period T_s can be deduced as follows:

$$P_{ij} = \frac{1}{T_s} \int_0^{T_s} v_{ac,i}'(t).i_{ij}(t)\, dt \quad (4)$$

$$= \frac{4}{\pi^3 f_s}. \sum_{\substack{k=1 \\ k\ odd}}^{\infty} \frac{1}{k^3}.\frac{V_i V_j}{n_{1i} n_{1j}}.\frac{1}{L_{ij}} \cos\left(k\frac{\alpha_i}{2}\right).\cos\left(k\frac{\alpha_j}{2}\right).\sin\left(k(\varphi_{1j} - \varphi_{1i})\right)$$

The total active power received by a port #i is therefore expressed by:

$$P_i = \sum_{\substack{j=1 \\ j\neq i}}^{n} P_{ji} \quad (5)$$

3 Calculation of Conduction Losses

The first targeted type of losses is the conduction losses in the copper wires and the conducting switches. The conduction losses of a port #i can be calculated as follows:

$$P_{cond,i} = \left(R_i + 2R_{ds,on}\right).{I_{i,rms}}^2 \quad (6)$$

R_i is the series resistance at port #i and $R_{ds,on}$ is that of a turned on switch, such that a maximum of two switches are turned on at once in each port. $I_{i,rms}$ is the RMS (Root Mean Square) value of the AC current flowing through port #i which's expression is deduced from (3) as follows:

$${I_{i,rms}}^2 = \frac{1}{T_s} \int_0^{T_s} {i_{L,i}}^2(t) dt \quad (7)$$

$$= \frac{4T_s}{{n_{1i}}^2.\pi^4}. \left[\frac{{V_i}^2}{{n_{1i}}^2}. \left(\sum_{\substack{j=1 \\ j\neq i}}^{n} \frac{1}{L_{ij}} \right)^2 .A(i,i) + \sum_{\substack{j=1 \\ j\neq i}}^{n} \left[\frac{{V_j}^2}{{n_{1j}}^2.{L_{ij}}^2}.A(j,j) \right] - 2. \left(\sum_{\substack{l=1 \\ l\neq i}}^{n} \frac{1}{L_{il}} \right). \sum_{\substack{j=1 \\ j\neq i}}^{n} \left[\frac{V_i V_j}{n_{1i}.n_{1j}}.\frac{1}{L_{ij}}.A(i,j) \right] + 2. \sum_{\substack{j=1,\, l=1 \\ j\neq i,\, l\neq i \\ j\neq l}}^{n} \left[\frac{V_j V_l}{n_{1j}.n_{1l}}.\frac{1}{L_{ij}L_{il}}.A(j,l) \right] \right]$$

Where:

$$A(i,j) = \frac{T_s}{2}. \sum_{\substack{k=1 \\ k\ odd}}^{\infty} \frac{1}{k^4}.\cos\left(k\frac{\alpha_i}{2}\right).\cos\left(k\frac{\alpha_j}{2}\right).\cos\left(k(\varphi_i - \varphi_j)\right)$$

4 Soft Switching Evaluation and Calculation of Switching Losses

A MAB converter is known to have a wide soft switching range [12]. However, when the system is operating at low power and/or when the DC links' voltages are perturbed, the risk of operating with hard switching increases. Switching losses can increase intensely when the soft switching is lost [12]. In this section, the ZVS (Zero Voltage Switching) criteria for each port are elaborated and the expression of the switching losses is developed accordingly.

4.1 Elaboration of the ZVS Criteria

Ideally, a switch is turned on at zero voltage (ZVS) if its drain current is negative during its switching instant. This negative current circulates through its anti-parallel body diode, turning it on, hence the voltage drop at the switch. Therefore, under an ideal scenario, the ZVS operation of a switch only depends on the direction of its current. Nevertheless, this condition is not sufficient in a practical converter. In fact, the parasitic capacitance C_{oss} between the drain and the source of the switch imposes a minimum amount of energy to be flowing through it during the switching instant in order to be charged or discharged. Therefore, a minimum current should be flowing through each port during its switching instants, assuming that the imposed dead time is sufficiently long for the energy exchange to take place completely. This energy value can be calculated using the Thevenin equivalent circuit of a port #i shown in Fig. *4*, and will be elaborated in this section [11].
The voltage source $V_{th,i}$ and the inductance $L_{th,i}$ replace the remaining ports of the MAB converter and are calculated from:

$$L_{th,i} = \frac{1}{\sum_{\substack{j=1 \\ j\neq i}}^{n} \frac{1}{L_{ij}}} \quad (8)$$

$$V_{th,i}(t) = \sum_{j=1, j\neq i}^{n} v_{ac,j}(t).\frac{L_{th,i}}{L_{ij}} \quad (9)$$

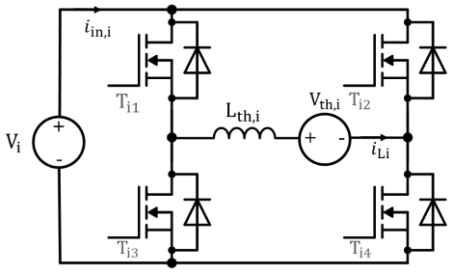

Fig. 4: Generic port-equivalent circuit of a MAB converter.

For each port, there are four switching instants in a switching period T_s. These instants are shown in Fig. *3* for a port #i and are denoted as: τ_{i1}, τ_{i2}, τ_{i1}' and τ_{i2}'. Since the current in each port is half-cycle symmetric, only two switching instants should be studied for each port: τ_{i1} and τ_{i2}. In each one of these instants, one switch is turned on and another switch is turned off. The switch that is being turned on is the switch where the ZVS conditions are examined. A soft switching (ZVS) will lead to nearly zero switching losses.

From Fig. *3*, the studied switching time instants of a port #i can be expressed in function of its phase shifts as follows:

$$\tau_{i1} = \left(\varphi_{1i} + \frac{\alpha_i}{2}\right).\frac{T_s}{2\pi} \tag{10}$$

$$\tau_{i2} = \frac{T_s}{2} + \left(\varphi_{1i} - \frac{\alpha_i}{2}\right).\frac{T_s}{2\pi} \tag{11}$$

If a port #i is operating in full-wave mode, i.e. if its internal phase shift is zero ($\alpha_i = 0$), it would only have two symmetrical switching instants ($\tau_{i2} = \frac{T_s}{2} + \tau_{i1}$), one of which should be studied (only τ_{i1} would be studied in this case).

4.1.1 Case 1: port #i with $\alpha_i > 0$: At time instant τ_{i1}, the AC voltage of port #i switches from $0V$ to $+V_i$. Switches T_{i3} and T_{i4} were ON before τ_{i1}, so switch T_{i3} is turned off and T_{i1} is turned on during τ_{i1} (Fig. *4*). Fig. *5* shows the equivalent circuit of port #i during switching instant τ_{i1} in this case. Switch T_{i3} is opened and T_{i1} is being closed. For the anti-parallel diode of T_{i1} to be turned on during τ_{i1}, the AC current $i_{L,i}(t)$ should be negative. The second current condition is derived from the minimum energy that should be circulating through port #i for the parasitic capacitances of the switches to be charged/discharged. Consequently, we can write from Fig. *5*:

$$i_{L,i}(\tau_{i1}) = -2.C_{oss}.\frac{dv_x}{dt} \tag{12}$$

$$i_{in,i}(\tau_{i1}) = \frac{i_{L,i}}{2} = -C_{oss}.\frac{dv_x}{dt} \tag{13}$$

The energy absorbed by the voltage sources can be expressed as follows [7], [11]:

$$E_{absorbed} = \int_{\tau_{i1}^-}^{\tau_{i1}^+} \left[V_{th,i}(\tau_{i1}).i_{L,i}(\tau_{i1}) - V_i.i_{in,i}(\tau_{i1})\right]dt$$

$$= \int_{\tau_{i1}^-}^{\tau_{i1}^+} \left[V_{th,i}(\tau_{i1}).\left(-2.C_{oss}.\frac{dv_x}{dt}\right) - V_i.\left(-C_{oss}.\frac{dv_x}{dt}\right)\right]dt$$

$$= \int_0^{V_i} \left[-2.C_{oss}.V_{th,i}(\tau_{i1}) + C_{oss}.V_i\right]dv_x$$

$$E_{absorbed} = -2.C_{oss}.V_{th,i}(\tau_{i1}).V_i + C_{oss}.{V_i}^2 \tag{14}$$

Where τ_{i1}^- and τ_{i1}^+ are the time instants right before and right after the switching instant τ_{i1}, respectively.

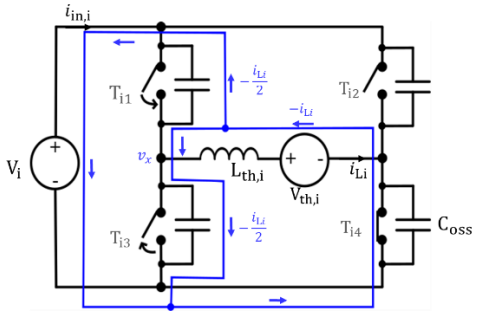

Fig. 5: Current circulation at port #i during switching instant τ_{i1} when $\alpha_i > 0$.

The minimum current value required for a soft turn on of switch T_{i1} during τ_{i1} can be written as:

$$\frac{1}{2}L_{th,i}.{i_{L,i}}^2(\tau_{i1}) \geq -2.C_{oss}.V_{th,i}(\tau_{i1}).V_i + C_{oss}.{V_i}^2 \tag{15}$$

So,

$$\left|i_{L,i}(\tau_{i1})\right| \geq \sqrt{2.\frac{C_{oss}.{V_i}^2}{L_{th,i}} - 4.\frac{C_{oss}.V_{th,i}(\tau_{i1}).V_i}{L_{th,i}}} \tag{16}$$

If $V_{th,i}(\tau_{i1}) > \frac{V_i}{2}$, ZVS is always achieved for a negative current $i_{L,i}(\tau_{i1})$.

At time instant τ_{i2}, the AC voltage of port #i switches from $+V_i$ to $0V$. Switches T_{i1} and T_{i4} were ON before τ_{i2}, so switch T_{i4} is turned off and T_{i2} is turned on during τ_{i2}. Fig. *6* shows the equivalent circuit of port #i during τ_{i2}. Switch T_{i4} is opened and T_{i2} is being closed. For the anti-parallel diode of T_{i2} to be turned on during τ_{i2} in this case, the AC current $i_{L,i}(t)$ should be positive.

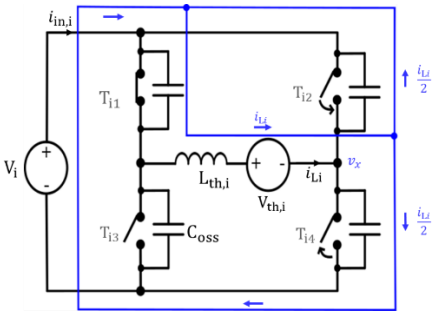

Fig. 6: Current circulation at port #i during switching instant τ_{i2} when $\alpha_i > 0$.

The minimum current value required for a soft turn on of switch T_{i2} during τ_{i2} can be written as:

$$\left|i_{L,i}(\tau_{i2})\right| \geq \sqrt{-2.\frac{C_{oss}.{V_i}^2}{L_{th,i}} + 4.\frac{C_{oss}.V_{th,i}(\tau_{i2}).V_i}{L_{th,i}}} \tag{17}$$

If $V_{th,i}(\tau_{i2}) < \frac{V_i}{2}$, ZVS is always achieved for a positive current $i_{L,i}(\tau_{i2})$. By symmetry, the satisfaction of the soft switching conditions at switching instants τ_{i1} and τ_{i2} means that all four switches of the studied port will turn on with ZVS.

4.1.2 Case 2: port #i with $\alpha_i = 0$: As explained before, the study of only one switching instant τ_{i1} is sufficient in this case. If the switching conditions at τ_{i1} are satisfied, all four switches of this port will turn on with ZVS.

At time instant τ_{i1}, the AC voltage of port #i switches from $-V_i$ to $+V_i$. Switches T_{i2} and T_{i3} are turned off at τ_{i1}, and T_{i1} and T_{i4} are turned on. Fig. *7* shows the equivalent circuit of port #i during τ_{i1} in this case. For the anti-parallel diodes of T_{i1} and T_{i4} to be turned on during τ_{i1}, the AC current $i_{L,i}(t)$ should be negative. We can write from Fig. *7*:

$$i_{L,i}(\tau_{i1}) = -2.C_{oss}.\frac{dv_x}{dt} \quad (18)$$

$$i_{in,i}(\tau_{i1}) = 0 \quad (19)$$

The minimum current value required during τ_{i1} will be:

$$\left|i_{L,i}(\tau_{i1})\right| \geq 2.\sqrt{-\frac{C_{oss}.V_{th,i}(\tau_{i1}).V_i}{L_{th,i}}} \quad (20)$$

If $V_{th,i}(\tau_{i1}) > 0$, ZVS is always achieved for a negative current $i_{L,i}(\tau_{i1})$.

ZVS occurs if both the current direction condition and minimum current value condition are simultaneously satisfied. Hard switching occurs if the current direction condition is not satisfied. However, if the current direction condition is respected, but the current value is smaller than the minimum required value, "an incomplete ZVS" occurs.

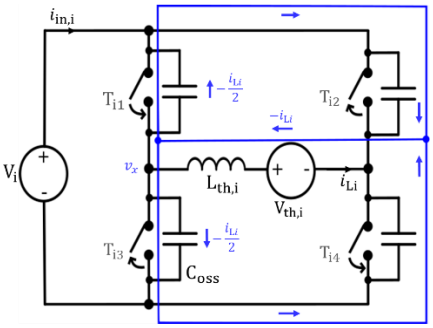

Fig. 7: Current circulation at port #i during switching instant τ_{i1} when $\alpha_i = 0$.

If a switch at a port #i undergoes an incomplete ZVS when it is switched on, its parasitic capacitance C_{oss} will not be fully discharged and a voltage ΔV will remain in it at the end of the switching instant. Similarly, the C_{oss} of its complementary switch will not be able to fully charge during its turning off and its final remaining voltage will be $(V_i - \Delta V)$ instead of V_i. Therefore, the remaining charge will be taken from the source, resulting in additional losses in the system [13].

The expression of the AC current during the switching instant can be written as:

$$i_{L,i}(t) = A_i.\cos(w_r t) + B_i.\sin(w_r t) \quad (21)$$

Where A_i and B_i are real constants calculated from the initial conditions of the switching instant $(i_{L,i}(0) = i_{L,i}(\tau_{i1})$ and $v_x(0) = 0)$ and $w_r = 2\pi f_r$, with f_r the resonance frequency of the LC circuit consisting of $L_{th,i}$ and the parasitic capacitances. When $i_{L,i}$ flows in the correct direction but is smaller than its minimum required value for a ZVS, $v_x = (V_i - \Delta V)$ will reach its maximum value at $t = t_{0i}$, such that $i_{L,i}(t_{0i}) = 0$. Instant t_{0i} can be calculated from (21) as following:

$$t_{0i} = \frac{1}{w_r}.\left[\arctan\left(-\frac{A_i}{B_i}\right) + \pi\right] \quad (22)$$

From (21), (22), figures 5, 6 and 7, voltage ΔV would be:

$$\Delta V = V_i - V_{th,i}(\tau_{i1}) \quad (23)$$
$$-L_{th,i}.(-A_{i1}.w_r.\sin(w_r.t_{0i1}) + B_{i1}.w_r.\cos(w_r.t_{0i1})) \quad for\ \alpha_i > 0 \text{ at } \tau_{i1}$$
$$\Delta V = V_{th,i}(\tau_{i2}) + L_{th,i}.(-A_{i2}.w_r.\sin(w_r.t_{0i2}) + B_{i2}.w_r.\cos(w_r.t_{0i2})) \quad for\ \alpha_i > 0 \text{ at } \tau_{i2}$$
$$\Delta V = \frac{1}{2}.[V_i - V_{th,i}(t_{di1}) - L_{th,i}.(-A_{i1}.w_r.\sin(w_r.t_{0i1}) + B_{i1}.w_r.\cos(w_r.t_{0i1}))] \quad for\ \alpha_i = 0 \text{ at } \tau_{i1}$$

Consequently, at the end of a switching instant, the final voltage value of the C_{oss} of a turning on switch will be:

$$V_{C_{oss},final} = \begin{cases} 0 & if\ ZVS\ occurs \\ V_i & if\ hard\ switching\ occurs \\ \Delta V & if\ incomplete\ ZVS\ occurs \end{cases} \quad (24)$$

4.2 Calculation of switching losses

The switching losses of a switch during turn on and turn off are expressed as follows [14]*:*

$$P_{ON} = \frac{V_D.I_D}{2}.t_{ON}.f_s \quad (25)$$

$$P_{OFF} = \frac{V_D.I_D}{2}.t_{OFF}.f_s \quad (26)$$

Where V_D and I_D are the drain-to-source voltage and current, respectively. t_{ON} is turn on time and t_{OFF} is the turn off time of the switch (from datasheet). For a port #i, we consider a function ZVS_{ik} to determine if the ZVS conditions at τ_{ik} elaborated in the previous section are satisfied, such that [7]:

$$ZVS_{ik} = \begin{cases} 1 & if\ both\ conditions\ at\ \tau_{ik}\ are\ satisfied \\ 0 & otherwise \end{cases} \quad (27)$$

The loss caused by the charge/discharge of the parasitic capacitance of a switch is calculated as follows, using (24):

$$P_{C_{oss}} = \frac{1}{2}.C_{oss}.V^2{}_{C_{oss},final}.f_s \quad (28)$$

For a port #i where $\alpha_i > 0$, the switching losses of port #i are calculated as follows, using (25), (26), (27) and (28):

$$P_{sw,i} = 2.[P_{ON}(\tau_{i1}) + P_{OFF}(\tau_{i1}) + P_{ON}(\tau_{i2}) + P_{OFF}(\tau_{i2})] + 2.P_{C_{oss}}(\tau_{i1}) + 2.P_{C_{oss}}(\tau_{i2})$$
$$= V_D(\tau_{i1}).(\tau_{i1}).f_s.[t_{ON}.(1 - ZVS_{i1}) + t_{OFF}] + V_D(\tau_{i2}).I_D(\tau_{i2}).f_s.[t_{ON}.(1 - ZVS_{i2}) + t_{OFF}] + 2.P_{C_{oss}}(\tau_{i1}) + 2.P_{C_{oss}}(\tau_{i2}) \quad (29)$$

Where:

$$V_D(\tau_{ik}) = V_i$$
$$I_D(\tau_{ik}) = \left|i_{L,i}(\tau_{ik})\right|$$

When $\alpha_i = 0$, the switching losses of port #i are calculated as follows:

$$P_{sw,i} = 4.[P_{ON}(\tau_{i1}) + P_{OFF}(\tau_{i1})] + 4.P_{C_{oss}}(\tau_{i1})$$
$$= 2.V_D(\tau_{i1}).I_D(\tau_{i1}).f_s.[t_{ON}.(1 - ZVS_{i1}) + t_{OFF}] + 4.P_{C_{oss}}(\tau_{i1}) \quad (30)$$

5 Proposed Efficiency Optimization Method

5.1 Minimization of the exchanged reactive power

By using the first harmonic approximation of a MAB converter's AC signals [12], [15] the reactive power exchanged between a port #i and a port #j would be:

$$Q_{ij} = \frac{8}{\pi^2 L_{ij} \omega_s} . \left[\left(\frac{V_i}{n_{1i}}\right)^2 . \cos^2\left(\frac{\alpha_i}{2}\right) - \left(\frac{V_j}{n_{1j}}\right)^2 . \cos^2\left(\frac{\alpha_j}{2}\right) \right] \quad (31)$$

When reactive power flows through a converter, the circulating currents increase and so do the losses of the system. Therefore, minimizing the reactive power exchange between ports will increase the system's efficiency at some operating points, especially at light loads because the reactive power's ratio from the total apparent power is higher when the active power is low. From (31), we can deduce that eliminating the reactive power exchange between ports can be done by achieving the following equality:

$$\frac{V_i}{n_{1i}} . \cos\left(\frac{\alpha_i}{2}\right) = \frac{V_j}{n_{1j}} . \cos\left(\frac{\alpha_j}{2}\right) \quad (32)$$

Completing this equality also means that the RMS values of the AC voltages' first harmonics of ports #i and #j are made equal. This could be interesting when voltage mismatches occur, as it compensates for the DC links' voltage variations and it could help re-establish the soft switching that can be lost due to these mismatches. A reference port is chosen for the internal phase shift values. In this paper, it will be port #1. Consequently, the internal phase shifts of all the other ports can be calculated based on port #1's internal phase shift value, using (32), as follows:

$$\alpha_i = 2 . arccos\left(\frac{V_1}{V_i} . n_{1i} . cos\left(\frac{\alpha_1}{2}\right)\right) \quad (33)$$

By using this method, the number of control degrees of freedom of the MAB will be reduced from $(2n-1)$ to (n), n being the total number of ports. The remaining control parameters will be the $(n-1)$ external phase shifts of the non-reference ports and the internal phase shift of the reference port. This will simplify solving the optimization problem aiming to minimize the total losses. In this proposed MPS modulation technique, the external phase shifts φ_i will be used for the active power flow control and the internal phase shift α_1 of the reference port for the loss minimization.

5.2 Minimization of total system losses

In this paper, the total losses of the MAB converter are considered equal to the sum of the conduction losses and the switching losses of all its ports. Other losses such as iron losses are neglected. Therefore, from (6), (29) and (30), we can write:

$$P_{total\ losses} = \sum_{i=1}^{n} P_{cond,i} + \sum_{i=1}^{n} P_{sw,i} \quad (34)$$

In order to choose the optimal value of α_1 using the proposed MPS modulation technique at a certain operating point, a sweep of this parameter between 0 and $\pi(rad)$ is completed using the developed GHA model. For each value of α_1 in this sweep, the internal phase shifts α_i of the remaining ports are calculated using (33) and their external phase shifts φ_i are calculated using (5), where P_i is equal to the desired power at port #i. The total system losses and number of soft switching switches are then calculated using the expressions developed in Sections 3 and 4, along with expression (34). An order of $k = 7$ is considered in the GHA model for all the expressions, except for the instantaneous current values used for the ZVS study, where $k = 101$ is used to get better precision. The value of α_1 leading to the optimal operation is retained with its corresponding φ_i values needed to satisfy the active power flow constraints.

Depending on the application in which the system is employed and on the priorities set by the user, this study can be used to define the optimal operation specifications. If achieving ZVS on all the system's switches were the priority, the optimal operation would correspond to the combination of control parameters where all the ZVS conditions are satisfied with the least possible losses. If maximizing the system's efficiency were the priority, even if hard switching may occur on certain switches, then choosing the combination where the total losses reach a global minimum value would be the optimal solution.

After that, the total losses and number of satisfied ZVS conditions at the retained optimum combination of the proposed MPS modulation are compared to those of when the classical EPS modulation is applied. This sets the boundary separating the operating points where the proposed MPS modulation method is beneficial from the ones where EPS modulation should be applied.

Finally, the calculated optimal internal and external phase shift values are fed forward to the MAB converter in order to update the PWM commands of its switches. Adding a feedforward will also decouple the dynamic control of the different ports (inverse matrix decoupling [16]). PI controllers will then correct the fed forward values of the external phase shifts φ_i in order to cancel the steady state error of the developed mathematical model.

Fig. *8* and Fig. *9* display the simulation results of the mathematical sweep of α_1 when applying the proposed MPS modulation technique on a four-port MAB converter at various power levels. Fig. *8* shows that using the proposed MPS modulation reduces total system losses compared to the classical EPS modulation, particularly at low loads. Furthermore, for each operating point, there exists one value of α_1 where these losses reach a global minimum. The presence of local minima in the total loss curve is caused by the saturation of certain internal phase shifts of the non-reference ports. These values cannot be negative or greater than π in radians. The existence of local minima demonstrates that a Perturb and Observe algorithm cannot achieve optimal operation. Fig. *9* demonstrates that the proposed MPS modulation also enables ZVS restoration at certain switches.

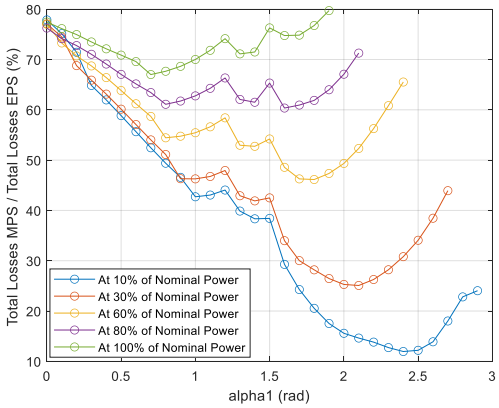

Fig. 8: Total loss percentage of the proposed MPS modulation in function of α_1 compared to EPS modulation applied in a QAB converter at different power levels.

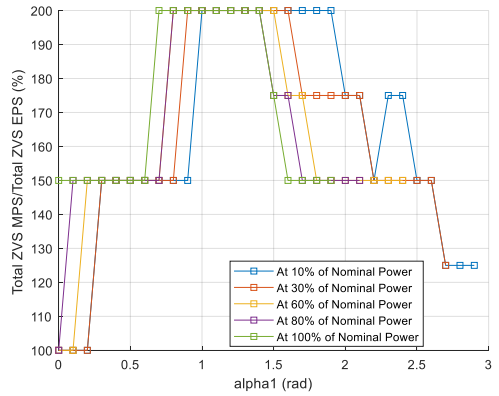

Fig. 9: Total number of ZVS switches percentage of the proposed MPS modulation as a function of α_1 compared to EPS modulation.

6 Experimental Results

A laboratory prototype QAB converter has been fabricated as shown in Fig. *10* and experimental results are represented in this section in order to validate the proposed optimized control strategy. The QAB prototype specifications are listed in Table 1. The proposed MPS modulation method is tested and compared to the conventional EPS modulation method at a low power operating point, with a maximum of 20% voltage distortion at its ports.

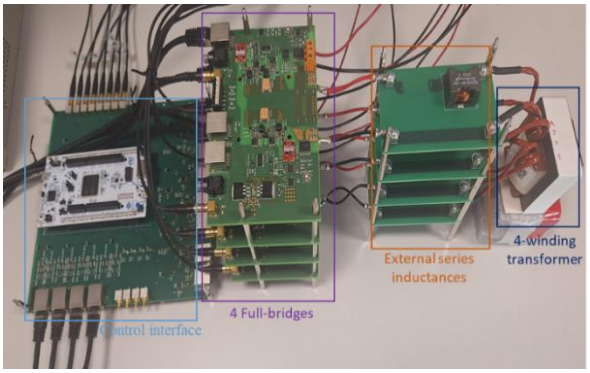

Fig. 10: QAB converter prototype.

The AC current and voltage waveforms at the different ports of the QAB converter prototype are displayed in Fig. 11. In Fig. 11(a), the conventional EPS modulation technique is used. In Fig. 11(b), the proposed control strategy is employed using the control parameters that correspond to the global minimum point of total system losses.

From Fig. 11, we deduce that the average RMS current flowing through each port at the chosen operating point is $I_{rms,i} = 1.1\ A$ when EPS modulation is applied, and is reduced to $I_{rms,i} = 462.5\ mA$ by using the proposed control strategy. In other words, the RMS current is reduced by approximatively 58% when the proposed MPS modulation is employed on this studied operating point. Additionally, it can be noticed from Fig. 11 that the ZVS is restored at ports 3 and 4, and ZCS (Zero Current Switching) occurs at the turning off switches when the MPS modulation is applied in this case. Peak AC currents are also reduced, which leads to less iron losses in the transformer and the inductors of the QAB converter.

The proposed control strategy was implemented on an STM32H743 microcontroller that achieves the mathematical sweep once every time the operating point changes and generates the optimal control parameter values in real-time.

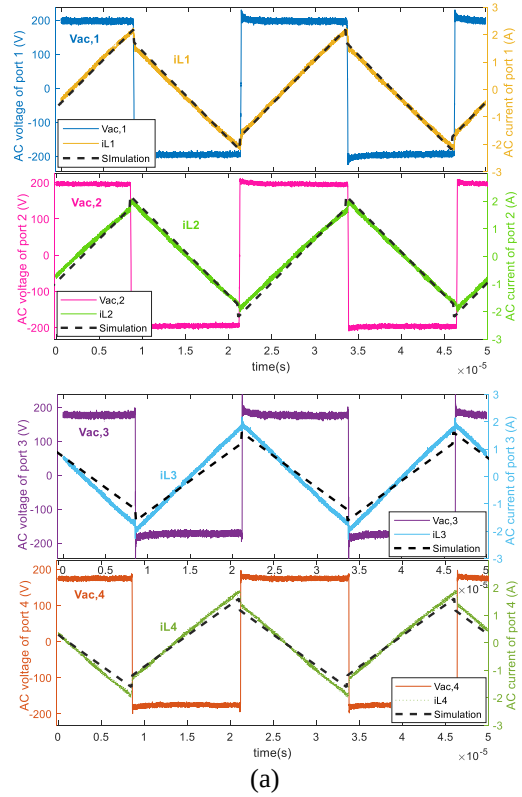

(a)

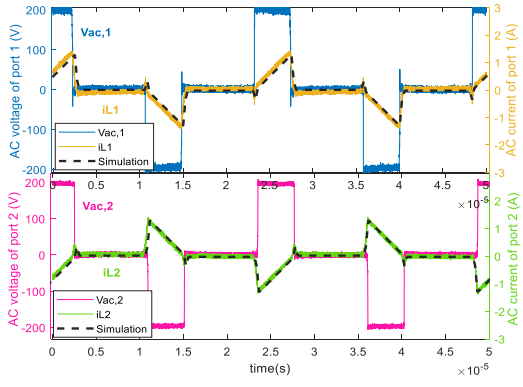

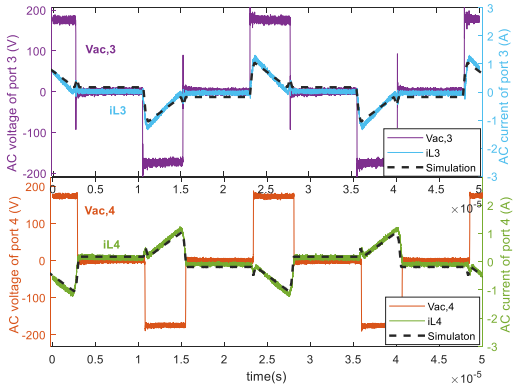

(b)

Fig. 11: Experimental and simulation results showing the AC current and voltage waveforms of each port when: (a) EPS modulation is applied; (b) the proposed MPS modulation is applied.

Table 1: Prototype parameters.

Parameter symbol	Parameter value
V_1, V_2, V_3, V_4	190 V, 190 V, 170 V, 170 V
f_s	40 KHz
$L_1 = L_2 = L_3 = L_4$	37 µH
$n_1 : n_2 : n_3 : n_4$	Turn ratio =1
$\|P_1\| = \|P_2\| = \|P_3\| = \|P_4\|$	40W
$\|P_{i,max}\|$	500W

7 Conclusion

In this paper, a novel efficiency-optimization strategy is proposed for a MAB converter. A GHA model is established for a MAB converter with n ports to predict the optimal values of the control parameters at each operating point. Conduction losses are decreased by limiting the reactive power exchange between the ports. Switching losses are decreased by ensuring a soft switching on the ports' switches. Experimental results are obtained from a built QAB converter prototype.

8 Reference

[1] S. Bandyopadhyay, P. Purgat, Z. Qin, and P. Bauer, "A Multiactive Bridge Converter With Inherently Decoupled Power Flows," *IEEE Trans. Power Electron.*, vol. 36, no. 2, pp. 2231–2245, Feb. 2021, doi: 10.1109/TPEL.2020.3006266.

[2] S. Galeshi, D. Frey, and Y. Lembeye, "Efficient and scalable power control in multi-port active-bridge converters," in *2020 22nd European Conference on Power Electronics and Applications (EPE'20 ECCE Europe)*, Lyon, France: IEEE, Sep. 2020, p. P.1-P.9. doi: 10.23919/EPE20ECCEEurope43536.2020.9215905.

[3] S. Galeshi, D. Frey, and Y. Lembeye, "Modular Modeling and Control of Power Flow in A Multi-Port Active-Bridge Converter," *Symposium De Genie Electrique, 3-5 July 2018, Nancy, France.*

[4] Y. Chen, P. Wang, H. Li, and M. Chen, "Power Flow Control in Multi-Active-Bridge Converters: Theories and Applications," in *2019 IEEE Applied Power Electronics Conference and Exposition (APEC)*, Anaheim, CA, USA: IEEE, Mar. 2019, pp. 1500–1507. doi: 10.1109/APEC.2019.8722122.

[5] T. Langbauer, A. Connaughton, F. Vollmaier, M. Pajnic, and K. Krischan, "Closed-Loop Control of a Three-Port Series Resonant Converter," in *2021 IEEE 22nd Workshop on Control and Modelling of Power Electronics (COMPEL)*, Cartagena, Colombia: IEEE, Nov. 2021, pp. 1–7. doi: 10.1109/COMPEL52922.2021.9646070.

[6] O. M. Hebala, A. A. Aboushady, K. H. Ahmed, and I. Abdelsalam, "Generalized Active Power Flow Controller for Multiactive Bridge DC–DC Converters With Minimum-Current-Point-Tracking Algorithm," *IEEE Trans. Ind. Electron.*, vol. 69, no. 4, pp. 3764–3775, Apr. 2022, doi: 10.1109/TIE.2021.3071681.

[7] S. Dey, A. Mallik, and A. Akturk, "Investigation of ZVS Criteria and Optimization of Switching Loss in a Triple Active Bridge Converter Using Penta-Phase-Shift Modulation," *IEEE J. Emerg. Sel. Topics Power Electron.*, vol. 10, no. 6, pp. 7014–7028, Dec. 2022, doi: 10.1109/JESTPE.2022.3191987.

[8] M. Shujun, G. Zhiqiang, and L. Yong, "Universal Modulation Scheme to Suppress Transient DC Bias Current in Dual Active Bridge Converters, IEEE transactions on power electronics, Vol. 37, No.2." Feb. 2022.

[9] J. Huang, Y. Wang, Z. Li, and W. Lei, "Unified Triple-Phase-Shift Control to Minimize Current Stress and Achieve Full Soft-Switching of isolated Bidirectional DC-DC converter, IEEE transactions in industrial electronics, Vol.63, No.7." Jul. 2016.

[10] F. Krismer, "Modeling and Optimization of Bidirectional Dual Active Bridge DC–DC Converter Topologies, PhD thesis, Power Electronic Systems Laboratory, ETH Zurich." 2010.

[11] P. Purgat, S. Bandyopadhyay, Z. Qin, and P. Bauer, "Zero Voltage Switching Criteria of Triple Active Bridge Converter," *IEEE Trans. Power Electron.*, vol. 36, no. 5, pp. 5425–5439, May 2021, doi: 10.1109/TPEL.2020.3027785.

[12] S. Galeshi, "'Cluster' converters based on multi-port active-bridge: application to smartgrids, Thesis at G2Elab - Université Grenoble Alpes." 2021.

[13] M. Kasper, R. Burkart, J. W. Kolar, and G. Deboy, "ZVS of Power MOSFETs Revisited," *Power Electronic Systems Laboratory, ETH Zurich, Physikstr. 3, 8092 Z¨urich, Switzerland*.

[14] G. Lakkas, "MOSFET power losses and how they affect power-supply efficiency," *Analog Applications Journal*, 2016.

[15] M. Blanc, Y. Lembeye, and J.-P. Ferrieux, "Dual Active Bridge (DAB) pour la conversion continu-continu," *Électronique*, Feb. 2019, doi: 10.51257/a-v1-e3975.

[16] C. Zhao, S. D. Round, and J. W. Kolar, "An Isolated Three-Port Bidirectional DC-DC Converter With Decoupled Power Flow Management," *IEEE Trans. Power Electron.*, vol. 23, no. 5, pp. 2443–2453, Sep. 2008, doi: 10.1109/TPEL.2008.2002056.